molecular pharmaceutics

pubs.acs.org/molecularpharmaceutics

Article

In Vitro and *In Vivo* Evaluation of the Pathology and Safety Aspects of Three- and Four-Way Junction RNA Nanoparticles

Kai Jin, You-Cheng Liao, Tzu-Chun Cheng, Xin Li, Wen-Jui Lee, Fengmei Pi, Daniel Jasinski, Li-Ching Chen, Mitch A. Phelps, Yuan-Soon Ho,* and Peixuan Guo*

Cite This: https://doi.org/10.1021/acs.molpharmaceut.3c00845

Read Online

ACCESS | Metrics & More | Article Recommendations | Supporting Information

ABSTRACT: RNA therapeutics has advanced into the third milestone in pharmaceutical drug development, following chemical and protein therapeutics. RNA itself can serve as therapeutics, carriers, regulators, or substrates in drug development. Due to RNA's motile, dynamic, and deformable properties, RNA nanoparticles have demonstrated spontaneous targeting and accumulation in cancer vasculature and fast excretion through the kidney glomerulus to urine to prevent possible interactions with healthy organs. Furthermore, the negatively charged phosphate backbone of RNA results in general repulsion from negatively charged lipid cell membranes for further avoidance of vital organs. Thus, RNA nanoparticles can spontaneously enrich tumor vasculature and efficiently enter tumor cells via specific targeting, while those not entering the tumor tissue will clear from the body quickly. These favorable parameters have led to the expectation that RNA has low or little toxicity. RNA nanoparticles have been well characterized for their anticancer efficacy; however, little detail on RNA nanoparticle pathology and safety is known. Here, we report the *in vitro* and *in vivo* assessment of the pathology and safety aspects of different RNA nanoparticles including RNA three-way junction (3WJ) harboring 2′-F modified pyrimidine, folic acid, and Survivin siRNA, as well as the RNA four-way junction (4WJ) harboring 2′-F modified pyrimidine and 24 copies of SN38. Both animal models and patient serum were investigated. *In vitro* studies include hemolysis, platelet aggregation, complement activation, plasma coagulation, and interferon induction. *In vivo* studies include hematoxylin and eosin (H&E) staining, hematological and biochemical analysis as the serum profiling, and animal organ weight study. No significant toxicity, side effect, or immune responses were detected during the extensive safety evaluations of RNA nanoparticles. These results further complement previous cancer inhibition studies and demonstrate RNA nanoparticles as an effective and safe drug delivery vehicle for future clinical translations.

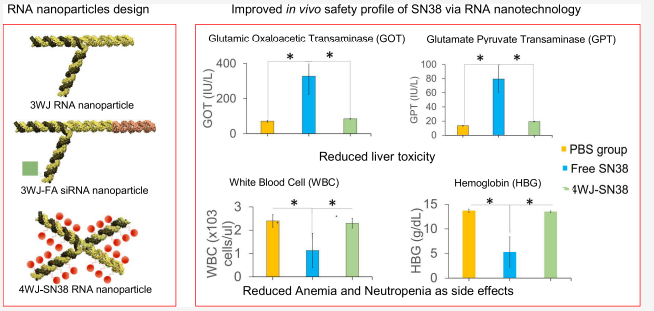

KEYWORDS: *RNA nanotechnology, pRNA 4WJ, pRNA 3WJ, CMC production, RNA pathology, RNA Safety, RNA immune response*

INTRODUCTION

Only 1.5% of the human genome codes for proteins, while the majority of the remaining 98.5% codes for small or long noncoding RNAs, demonstrating its biological importance. RNA can serve either as a therapeutic that is delivered or as a substrate targeted by drugs. In recent years, RNA has gained focus in pharmaceutic and vaccine field, most notably through the FDA approval of RNA-based therapeutics[1−3] and authorization of mRNA COVID-19 vaccines.[4−7] These approvals confirm the safety and stability of RNA in clinical applications.[8−11] RNA therapeutics have now emerged as a prominent field and is becoming the third milestone in pharmaceutical drug development.[12−19]

RNA nanotechnology, similar to the system of Lego,[13] is to deal with the self-assembling of nanometer-scale structures composed mainly of RNA.[20−29] RNA nanoparticles can serve as therapeutics or drug delivery vehicles to cancers with strong inhibition.[15,30−38] RNA nanoparticle-based drug delivery systems exhibit several advantages, including efficient and spontaneous accumulation in tumors, improved pharmacokinetics, and the undetectable gross toxicity and low immune responses.[25,31,39−44] These features also facilitate the repeated treatment of chronic diseases. It was found that RNA nanoparticles can be stretched or released over multiple rounds of repeats much like rubber[45] and this stretching is important for the beneficial *in vivo* features. Furthermore, RNA naturally exhibits elasticity, deformation, and motility, making it highly promising for spontaneous targeting toward cancer vasculature and fast excretion through the kidney glomerulus

Received: September 15, 2023
Revised: December 8, 2023
Accepted: December 11, 2023

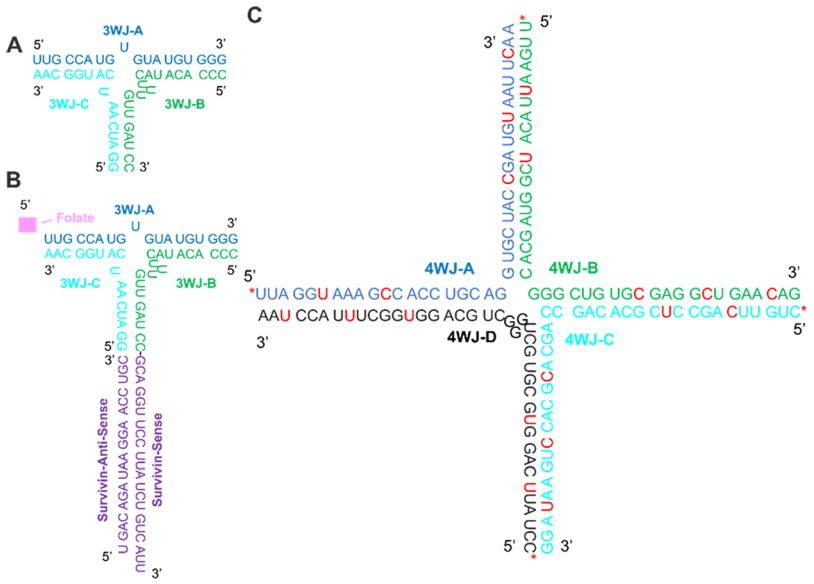

Figure 1. RNA nanoparticle designs. Schematic diagram with sequences of (A) 3WJ, (B) 3WJ-FA-siRNA, and (C) 4WJ-24 SN38 copies of RNA nanoparticles. Red characters indicate SN38-conjugated nucleotide. * Characters indicate 5′ end-conjugated SN38.

to urine.[13,45] RNA nanoparticles exhibit rubber-like properties,[45−47] making them highly attractive as potential cancer therapeutics.

Our team has created multifunctional, ultrastable RNA complexes with uniform nanoscale size, controllable structure, and precise stoichiometry, including Phi29 3WJ[31] and 4WJ.[10] These branched RNA nanoparticles offer multivalency and can be conjugated to chemical drugs for controlled delivery to the tumor microenvironment.[10,31,33,48] These nanoparticles have proven great potential as cancer therapeutics by demonstrating specific tumor accumulation, delivery of therapeutics resulting in apoptosis, and initial safety with no gross toxicity. However, further data is necessary to overcome existing challenges and maximize RNA nanoparticle's clinical benefits. It will be beneficial to evaluate in-depth the pathology, side effects, and toxicity of these RNA nanoparticles.

In this study, we aim to further prove the capability of RNA nanoparticles for cancer treatments by providing detailed pathology and safety parameters. 3WJ and 4WJ nanoparticles with and without chemotherapeutic conjugates (Figure 1) were evaluated *in vitro* and *in vivo*, including hemolysis study, platelet aggregation study, complement activation study, plasma coagulation study, interferons induction study, animal organ weight, H&E staining, serum biochemistry, and hematological study. Extensive evaluations revealed that these 3WJ and 4WJ RNA nanoparticles with and without drug conjugation did not have detectable toxicity, side effects, or immune responses. In general, the RNA nanoparticles provided safe profiles to serve as a viable drug delivery vehicle. In combination with the strong tumor inhibition of previous studies, there is a strong rationale to more toward the translation of RNA nanoparticles.

MATERIALS AND METHODS

Design and Preparation of RNA Nanoparticles. Multifunctional RNA nanoparticles were designed and constructed via bottom-up self-assembly approaches. The 3WJ nanoparticle is composed of three RNA fragments harboring 3WJ-A, 3WJ-B, and 3WJ-C strands. The three-way junction-folic acid-Survivin siRNA RNA nanoparticles (3WJ-FA-siRNA) contained four RNA fragments harboring 3WJ-A-folate, 3WJ-B-Survivin sense, 3WJ-C, and Survivin antisense. The four-way junction SN38-conjugated RNA nanoparticles (4WJ-SN38) contained four RNA fragments, including (1) 4WJ-A-6 SN38, (2) 4WJ-B-6 SN38, (3) 4WJ-C-6 SN38, and (4) 4WJ-D-6 SN38. RNA sequences can be found in the Supporting Information.

RNA strands were synthesized chemically using solid-phase synthesis. 2′-Fluoro (2′-F) modified cytosine (2′F−C) and uracil (2′F−U) nucleotides were incorporated into all RNA strands except the Survivin antisense stand for improving thermostability and nuclease resistance of the RNA nanoparticles. SN38 was conjugated to RNA strands via click chemistry between Drug-Azido and RNA-6 alkyne using methods previously published.[10,37]

After synthesis, RNA component strands were purified by ion-pair reversed-phase HPLC to remove salts, incomplete synthesis strands, or unconjugated chemicals. All RNA nanoparticles were prepared via thermocycler annealing via rapid heating to 95 °C to denature all secondary structures, followed by slow cooling down to 4°.

Analysis Hemolytic Properties of Nanoparticles. Hemolysis tests were performed *in vitro* using the NCL protocol ITA-1.[49] First, fresh human blood was treated with lithium heparin to prevent clotting and was diluted using PBS into 10 mg/mL of total hemoglobin. Then, the diluted sample was combined with the experimental materials and incubated at 37 °C for 3h. After incubation, the cell-free liquid was processed, and the hemoglobin that was not bound to plasma was assessed by converting the hemoglobin and its metabolites into cyanmethemoglobin (CMH) with Drabkin's reagent for measurement. The quantification of CMH was then carried out against a hemoglobin standard by measuring the sample absorbance at 540 nm. The rate of hemolysis was determined as $\%\ \text{of Hemolysis} = \frac{\text{hemoglobin in the test sample}}{\text{TBHd}} \times 100$, where TBHd refers to the total blood hemoglobin diluted.

There are alternative versions of the hemolysis test accessible. These procedures do not involve converting

https://doi.org/10.1021/acs.molpharmaceut.3c00845
Mol. Pharmaceutics XXXX, XXX, XXX−XXX

hemoglobin to its enduring CMH state. Instead, they gauge the level of hemolysis by examining oxyhemoglobin at one of its main absorption points, specifically at the wavelength of 415, 541, or 577 nm.[50]

Analysis of Platelet Aggregation. The platelet aggregation tests were conducted *in vitro* according to the NCL protocol ITA-2.2.[51] Whole human blood was collected in sodium citrate tubes and then centrifuged to obtain platelet-rich plasma (PRP) and platelet-poor plasma (PPP). The PRP was mixed with test samples and the ChronoLum reagent and incubated at 37 °C for 6 min in a platelet aggregation profiler to measure whether RNA nanoparticles may induce platelet aggregation. Additionally, the PRP was mixed with the test samples, ChronoLum reagent, and collagen and incubated at 37 °C for 6 min in a platelet aggregation profiler to measure whether RNA nanoparticles may block the platelet aggregation caused by collagen. Collagen (100 μg/mL)-mixed PRP was used as a positive control, PPP alone was used as a negative control, and nontreated PRP runs were internal test controls. A positive response was determined by a platelet aggregation of >20%. The ChronoLum reagent was employed for tracking ATP release from platelets, providing an extra measure to verify that alterations in light transmission were indeed a result of platelet aggregation. The ChronoLog aggregometer was used to determine sample turbidity. However, a definition of PRP and PPP based on platelet quantification would be more helpful to obtain a more precise result.

The aggregation percentage was determined using the following formula $\%\ \text{Aggregation} = \frac{\text{AUC sample}}{\text{AUC positive}} \times 100$.

Analysis of Complement Activation on RNA Nanoparticles. *In vitro* tests were carried out to measure complement activation using the NCL protocol ITA-5.2.[52] Plasma was extracted from recently drawn human blood and mixed with test samples, and the cobra venom factor (CVF) was used as a positive control. After a 30-minute incubation at 37 °C, the samples were examined using a commercial enzyme immunoassay kit to detect the iC3b component of the complement. The RNA nanoparticles were assessed at four RNA concentrations (0.14, 0.72, 3.6, and 35.6 μg/mL) while Doxil, a commercially relevant nanoparticle, was used as a positive control.

Plasma Coagulation Test. The NCL ITA-12[53] method was used to perform this assay. Initially, human blood was collected in tubes containing sodium citrate. After centrifuging the blood at 2500 *g* for 10 min, plasma was collected. The samples were then incubated with plasma in a microcentrifuge tube for 30 min at 37 °C and subsequently centrifuged at 17,000 *g* for 5 min. The STA-R Evolution coagulometer (Diagnostica Stago) was used to measure activated partial thromboplastin time (APTT), prothrombin time (PT), and thrombin time after exposure. Nontreated plasma, PBS, and abnormal control plasma were utilized as untreated, negative control, and positive control, respectively.

The standard coagulation time for the PT assay is 13.4 s or less, APTT is 34.1 s or less, and thrombin assay is 21 s or less. Abnormal control plasma should have coagulation times above these limits.

Interferon and Cytokine Induction Assay. The NCL method ITA-10,[54] ITA-25,[55] and ITA-27[56] were used to conduct this assay. In short, human PBMCs were suspended in RPMI 1640 medium containing 10% FBS. The cells were then exposed to samples and incubated at 37 °C for 24 h. Positive and negative controls were lipopolysaccharides (LPS) at 20 ng/mL and PBS, respectively. After exposure, the supernatants were collected and underwent centrifugation at 12,000 rpm for 15 min. ELISA kits were used to measure interferon type I (IFN α, β, and ω), type II (IFN γ), and type III (IFN λ).

Treatment Plan of Different RNA Nanoparticles. All animals were kept at the National Defense Animal Center according to the protocol approved by the Association for Laboratory Animal Care Evaluation and Certification (LAC-101−0064). A549 lung cancer cells were utilized to establish xenograft models in male nonobese diabetic-severe combined immunodeficiency-IL2R gamma null (NSG) mice. The cells were transplanted into the dorsal region of 4−5 weeks-old mice. Once the tumor size reached 100 mm^3, the mice bearing A549 xenografts were randomly allocated into three groups: PBS, SN38 free drug, and 4WJ-SN38, with each group consisting of five mice. To assess the efficacy of the treatments, samples were administered intravenously (IV) through tail-vein injections. The dose was set at 2 mg/kg, and five injections were given on days 1, 3, 5, 7, and 9. The dosage used for the 4WJ-24 SN38 RNA nanoparticles *in vivo* safety experiments was also 2 mg/kg (Xin Li and Peixuan Guo, unpublished results). The negative control group received PBS injections. The tumor size was monitored every 2 days throughout the treatment period, and the volume was calculated using the formula (length × width^2)/2. A two-tailed unpaired *t* test was used as statistical analysis to compare the different treatment groups. The results are reported as mean ± SEM, with significance levels denoted as $^*p < 0.05$.

Organ Weight Measurement. After the *in vivo* delivery of RNA nanoparticles, all animals, including tumor-bearing mice and healthy mice, were euthanized. The major organs, namely the liver, spleen, kidney, heart, and lung, were excised and harvested from the sacrificed mice. The organs were weighed directly using an electronic balance. The organ weight data are expressed as mean ± SEM. Statistical analysis of the organ weights was performed using a two-tailed *t* test. Significance levels are indicated as $^*p < 0.05$.

H&E Staining. After weighing major organs from the sacrificed mice, organs were subjected to fixation in 4% paraformaldehyde, embedding, and sectioning processes to generate formalin-fixed, paraffin-embedded (FFPE) sections. H&E staining was performed on the FFPE sections. Hematoxylin dye was used to impart a blue color to the cell nuclei, while eosin dye was employed to stain the cell cytoplasm and extracellular matrix pink. The H&E-stained sections were directly captured using a light microscope at 10× magnification.

Analysis of Serum Biochemistry in the Treated NSG Mice. After *in vivo* delivery of RNA nanoparticles, cardiac blood was collected from each NSG mouse, including both the treated and healthy control groups, using a cardiac puncture. The collected blood was then divided into two parts. One part was utilized for whole blood hematological analysis, while the other was centrifuged at 1200 *g* for 10 min to obtain serum for biochemical analysis. Hematological and biochemical analyses were performed at TMU Hospital following standard protocols. The hematological analysis was conducted using the Beckman Coulter DxH 800 automated hematology analyzer. The biochemical analysis used the Roche Cobas c702 analyzer. Statistical analysis of the data was performed using a two-tailed unpaired *t* test. The results are presented as mean ± SEM. Significance levels are denoted as $^*p < 0.05$.

https://doi.org/10.1021/acs.molpharmaceut.3c00845
Mol. Pharmaceutics XXXX, XXX, XXX−XXX

Analysis of Hematology of the Treated NSG Mice. All animals, including tumor-bearing mice, were included in the study. The data obtained are presented as mean ± SEM values. Cardiac blood samples were collected from each NSG mouse at the end point of the treatment for hematological analysis. Statistical analysis of the organ weight data was performed using a two-tailed *t* test. Significance levels are denoted as $*p < 0.05$.

Statistics. The experiment was conducted multiple times, ensuring a minimum of three repetitions for each sample tested. The results are reported as the mean value accompanied by the standard error of the mean (SEM), unless stated otherwise. Statistical analysis of mean differences was performed using GraphPad software, employing the unpaired *t* test. A significance level of $p < 0.05$ was used to determine statistical significance.

RESULTS

Design and Quality Check of RNA Nanoparticles. Two 3WJ RNA nanoparticles were designed based on our previous published results (Figure 1A,B).[31] The first nanoparticle was a 3WJ scaffold with pyramidines modified with fluorine at the 2′ location (Figure 1A). The second nanoparticle is a 2′F 3WJ scaffold with the 3WJ-A strand 5′ end modified with folic acid (FA), the 3WJ-B strand 5′ end extended with the sense strand of Survivin (BRCCA1) siRNA, the 3WJ-C strand, and the Survivin (BRCCA1) antisense strand (Figure 1B). No bacterial contamination was detected in either 3WJ or 3WJ-FA-siRNA nanoparticle samples, and endotoxin levels were below the endotoxin limit (EL) for both samples (Figure S1). The selection of the nanoparticle and RNA nanoparticle concentration used in the *in vitro* experiments is a follow-up of our past pharmacological characterization research.[9] In that research, the RNA nanoparticles did not induce interferon response *in vitro* at a concentration of 4ug/mL. A further investigation on the hemolysis, platelet aggregation, plasma coagulation, complement activation, and interferon (IFN) induction profile of the RNA nanoparticles is in reference to the concentrations as reported before.[9]

We also previously designed a 4WJ RNA nanoparticle to carry different chemotherapeutics.[10] For 4WJ-24 SN38 RNA nanoparticles (Figure 1C), 4WJ A, 4WJ B, 4WJ C, and 4WJ D RNA strands were modified with (A) 2′F modified pyrimidines to result in nuclease resistance and (B) 2′-O-propargyl amidites to replace 6 bases on each 4WJ-A, B, C, and D strands for the click chemistry. SN38-N_3 was then conjugated to bases with a 2′-O-propargyl group via the click reaction (Figure 1C). 4WJ-A-SN38, 4WJ-B-SN38, 4WJ-C-SN38, and 4WJ-D-SN38 are purified via RP-HPLC.

Following the synthesis of component strands of both the 3WJ and 4WJ, the RNA nanoparticles were assembled through controlled thermocycling. Each of the three RNA nanoparticles is assembled in a one-pot single step with high efficiency. Polyacrylamide native gels confirmed RNA nanoparticle stepwise formation (data not shown) as previously published with similar nanoparticles.[10,31] As a result, stable RNA nanoparticles were created with and without chemotherapeutics or siRNA to act as drug delivery vehicles. Our prior testing of these nanoplatforms has demonstrated significant inhibition in tumor growth in triple-negative breast cancer,[10] prostate cancer,[41] colorectal cancer,[57] and more.

Hemolysis Study on RNA Nanoparticles. Assaying interactions of RNA nanoparticles with blood components, specifically with red blood cells, is of importance as RNA nanoparticles are best delivered intravenously and have the ability to continually interact with blood components until reaching the tumor microenvironment. Nanoparticles interacting with blood have resulted in significant toxicities and negative implications for clinical translation.[58,59] However, information about the interaction of RNA nanoparticles with red blood cells is minimal. Therefore, a hemolysis study of the RNA nanoparticles was carried out to determine whether RNA nanoparticles can cause red blood cell destruction. The hemolysis study is the starting point to evaluate the interaction between RNA nanoparticles and red blood cells. Compared to the positive control group triggered by Triton X-100, hemolysis of 3WJ nanoparticles was below the limit of detection (BLOD) in a concentration ranging from 0.14 to 3.6 μg/mL siRNA equivalent same as the negative control PBS group (Figure 2A). Similar to 3WJ nanoparticles, 3WJ-FA-siRNA RNA nanoparticles show the same result without the hemolysis phenomenon after administration (Figure 2B), and folic Acid or siRNA clearly did not trigger hemolysis. This result clearly indicates the safety when administrating our RNA nanoparticles, and RNA nanoparticles alone or RNA nanoparticles with targeting and therapeutic groups clearly did not affect the integrity of human red blood cells at any of the tested concentrations.

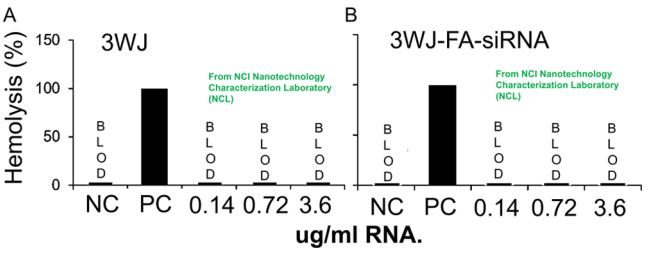

Figure 2. Hemolysis study of RNA nanoparticles. Hemolysis data of (A) 3WJ nanoparticles and (B) 3WJ-FA-siRNA nanoparticles. BLOD = below the limit of detection. NC is a negative control. PC is positive control.

Platelet Aggregation and Coagulation Study on RNA Nanoparticles. Nanoparticles come in contact with the platelets within the blood after administration and may cause platelet activation and aggregation.[60,61] Serious bleeding or thrombosis phenomenon caused by interference with normal platelet function may risk patients' lives. RNA nanoparticles have been used *in vivo* without causing blood aggregation, but their overall safety profile on platelet activation and aggregation is limited. As a result, understanding the interaction between platelets and RNA nanoparticles is critical for translational medicine. Compared to the positive control group triggered by collagen, both 3WJ and 3WJ-FA-siRNA RNA nanoparticles did not induce platelet aggregation itself (Figure 3A,B) and did not inhibit collagen-induced aggregation (Figure 3C,D) at any of the tested concentrations. This result clearly indicates the safety when administrating our RNA nanoparticles, and RNA nanoparticles alone or RNA nanoparticles with targeting and therapeutic groups clearly did not have blood aggregation concerns.

Plasma Coagulation Study on RNA Nanoparticles. Apart from red blood cells and platelets, nanoparticles may interact with many other protein components within the plasma.[62] The published information on the plasma coagu-

https://doi.org/10.1021/acs.molpharmaceut.3c00845
Mol. Pharmaceutics XXXX, XXX, XXX−XXX

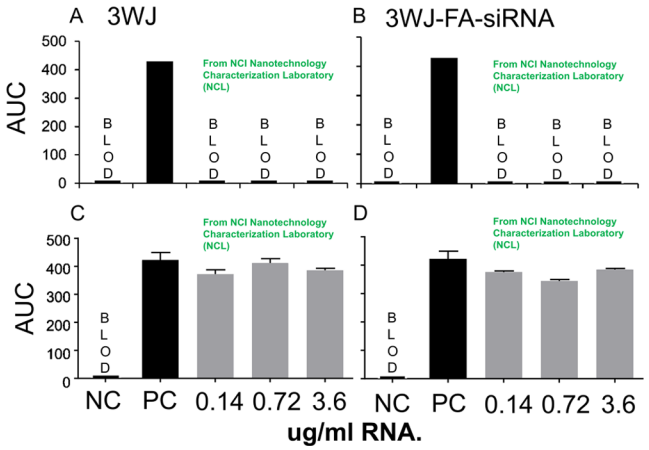

Figure 3. Platelet aggregation study of RNA nanoparticles. Platelet aggregation data of (A) 3WJ nanoparticles alone or (B) 3WJ-FA-siRNA nanoparticles alone and (C) 3WJ nanoparticles or (D) 3WJ-FA-siRNA nanoparticles together with collagen. BLOD = below limit of detection. NC is negative control. PC is positive control.

lation profile of RNA nanoparticles is limited. A blockage of important coagulation factors within plasma could be dangerous, as it might increase the coagulation time. As a result, the plasma coagulation test could be a valid tool to understand the overall safety profile after RNA nanoparticles are administered into the body. Compared to the negative control and untreated group, both groups of nanoparticles did not affect plasma coagulation time *in vitro* under the tested conditions (Figure 4). Prolongation of the plasma coagulation time samples that were exposed to nanoparticles suggests that these test particles either deplete or inhibit the coagulation factor, and both 3WJ

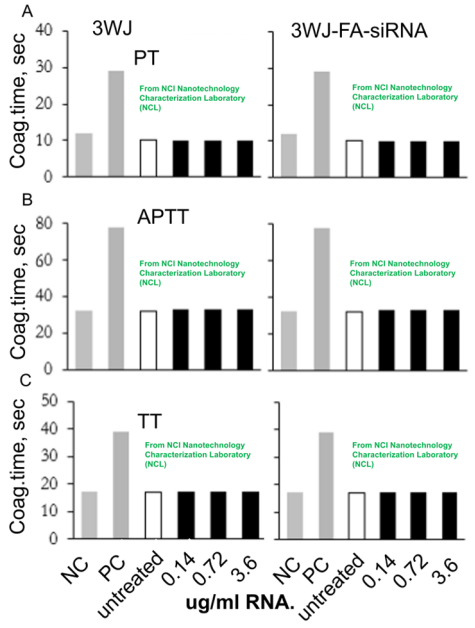

Figure 4. Plasma coagulation data on both 3WJ and 3WJ-FA-siRNA nanoparticles. (A) Prothrombin time of RNA nanoparticles. (B) Activated partial thromboplastin time of RNA nanoparticles. (C) Thrombin time of RNA nanoparticles. PT = Prothrombin time. APTT = Activated partial thromboplastin time. TT = Thrombin time. Coag.time = Coaggregation time. NC is negative control. PC is positive control.

and 3WJ-FA-siRNA RNA nanoparticles clearly do not inhibit coagulation factors as tested (prothrombin time, activated partial thromboplastin time, and thrombin time). This result clearly indicates the safety when administrating our RNA nanoparticles, and RNA nanoparticles alone or RNA nanoparticles with targeting and therapeutic groups clearly did not trigger plasma coagulation issues at any of the tested concentrations.

Complement Activation Study on RNA Nanoparticles. Complement activation can be caused by some nanoparticles[63] like PEGylated nanoparticles.[64] The activation can cause acute inflammatory reactions and chronic Immunol responses,[63] and both may cause concerns about patients' safety and the therapeutic efficacy of nanoparticles. An investigation of the *in vitro* complement activation against RNA nanoparticles is a critical part to understanding the overall immune response profile. Compared to the positive control group triggered by the cobra venom factor (CVF) and Doxil, weak activation of the complement (about 2-fold above baseline) of ic3b was detected in 3WJ nanoparticle-treated plasma at the highest tested concentration (Figure 5A).

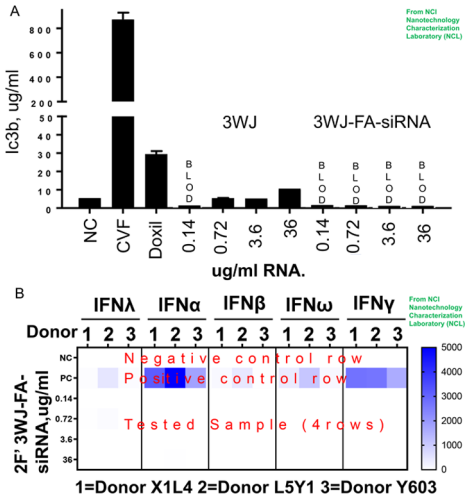

Figure 5. Immunogenicity profiles of RNA nanoparticles (A) Complement activation data on 3WJ and 3WJ-FA-siRNA nanoparticles. BLOD = below limit of detection. NC is negative control. CVF = Cobra Venom Factor. (B) Interferon (IFN) induction data of 3WJ-FA-siRNA RNA nanoparticles.

However, the observed activation was more than 50% below that induced by Doxil, which is known to cause CARPA in sensitive patients in the clinic. The rest of the concentrations were undetectable or similar to the negative control group. Complement activation was not detected in plasma treated with 3WJ-FA-siRNA RNA nanoparticles even at the highest tested concentration (Figure 5A). Herein, we believe that the immunogenicity of our RNA nanoparticles is relatively low.

Interferon Induction by RNA Nanoparticles. The human body targets and destroys foreign materials through immune responses. Cytokines and chemokines, including interferons, are induced and secreted by the immune system, resulting in inflammation and destruction of foreign materials, primarily viral components. Viral RNA has shown to induce cytokine responses;[65] however, our previous results revealed that cytokine responses toward RNA nanoparticles are limited,[9] and the intensity of immune response to RNA nanoparticles is tunable based on the size, shape, and

https://doi.org/10.1021/acs.molpharmaceut.3c00845
Mol. Pharmaceutics XXXX, XXX, XXX−XXX

sequence.[8,66] It is important to further demonstrate that our RNA nanoplatform is capable of being safe in cytokine responses and specifically not in induced interferon responses. Here, the 3WJ nanoparticles were tested for interferon induction using blood from three different human donors. Compared to the negative control which is inducted by PBS and positive control which is inducted by either the cobra venom factor or Doxil, the induction of all three types of interferons, type I (IFN α, β, and ω), type II (IFN γ), and type III (IFN λ), was evaluated on 3WJ-FA-siRNA nanoparticles. The induction of all interferons was detected in the positive control samples on every individual donor; however, IFN α, β, ω, and γ inductions are not detected in 3WJ-FA-siRNA-treated patient samples (Figure 5B), which is similar to the negative control group. Limited IFN λ induction was detected in one donor group only at a relatively low administration concentration (0.72 μg/mL) (Figure 5B) in the 3WJ group, and we expect that is due to heterogeneous response between individual donors. These results match with our past findings that RNA nanoparticles have limited IFN induction.[9]

***In Vivo* Safety Profile of SN38-Conjugated RNA Nanoparticles: A Case Study.** SN-38 is an active metabolite of the topoisomerase I inhibitor Irinotecan, and SN-38 can inhibit both DNA and RNA synthesis. However, SN38 itself may cause adverse effects including severe diarrhea, myelosuppression, and neutropenia.[67] SN38 was a case study to understand the overall safety profile of RNA nanoparticles carrying chemotherapeutics while examining organ function and assayed for interactions with blood and organs. On a gross level of toxicity, organ weight change upon RNA nanoparticles carrying SN38 delivery was carried out. Heart, lung, or kidney weight changes were not observed compared to the PBS control group (Figure 6A). Reduced spleen weight and increased liver weight were observed in the 4WJ-SN38 group compared to the PBS group, which may contribute to the toxic nature of SN38 itself (Figure 6A). To further investigate possible organ toxicities and to explain liver and spleen weight changes, H&E staining was used to examine possible lesions caused by RNA nanoparticles carrying chemotherapeutics. H&E staining is the histological assay combining hematoxylin and eosin. The H (hematoxylin) stains cell nuclei into a purplish-blue color, and E (eosin) stains the extracellular matrix and cytoplasm into a pink color with other structures displaying different shades. Interestingly, no obvious tissue-level lesions were found in the 4WJ-SN38 treatment groups when compared to the PBS control group (Figure 6B). Drug toxicity may cause necrotic and karyolysis cells that will show up in H&E staining.[68] Our data revealed that the morphology of cell nuclei is similar between both the PBS and 4WJ-SN38 treatment groups, and the unchanged nuclear morphology may indicate the limited amount of karyolysis. The cytoplasmic component distribution changes can be used to indicate necrotic regions. No significant changes were detected in the 4WJ-SN38-treated and PBS control groups.

Following 4WJ conjugated with SN38 delivery to mice, serum biochemistry studies were completed to examine its compatibility with organ functionality. Serum biochemistry results showed that free SN38 significantly increased the level of glutamic oxaloacetic transaminase (GOT) and glutamate pyruvate transaminase (GPT), but 4WJ-SN38 did not increase these two transaminases (Figure 7A). Both GOT and GPT elevated levels indicate a possible sign of liver damage, confirming liver toxicity as a common adverse effect from

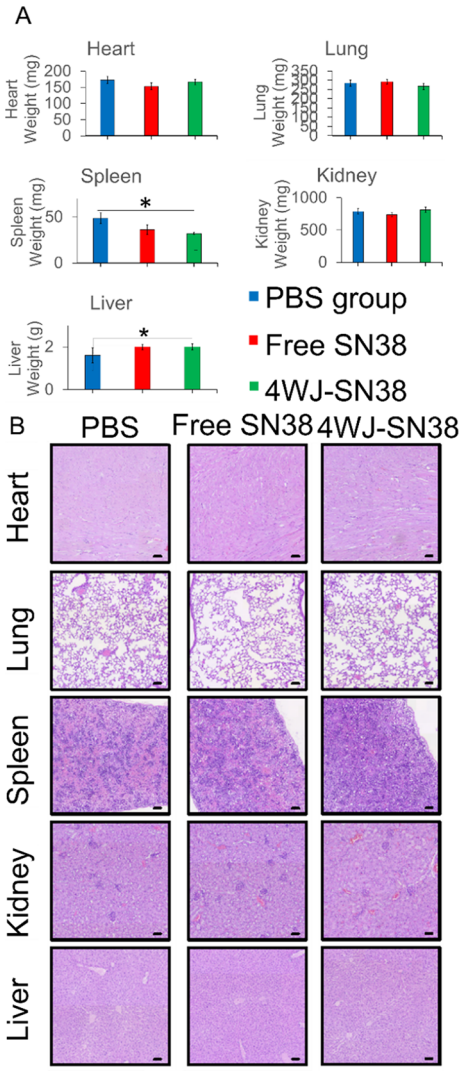

Figure 6. *In vivo* organ level study of the safety profile of 4WJ-SN38. (A) Organ weights study (B) H&E staining of major organs. *P < 0.05.

free SN38.[69] Furthermore, the lactate dehydrogenase (LDH) levels were also observed to increase comparing the SN38 free drug group with the PBS control group, and increased LDH level may indicate tissue damage.[70] SN38-carried RNA nanoparticles may mitigate tissue damage caused by SN38 (Figure 7A). Using 4WJ-SN38 may overcome liver toxicity and tissue damage, which is an advantage of using RNA nanoparticles to deliver chemotherapeutics. Hematological results further demonstrated that the white blood cell, platelet, hemoglobin, and mean corpuscular hemoglobin concentration levels are significantly reduced for the SN38 free drug group compared to the PBS control group, while the 4WJ-SN38 group shows negligible effect (Figure 7B). The reduction of WBC and platelets matches other groups' findings when administering SN38,[71] and the reduction of the hemoglobin level is a common indication of anemia when administering chemotherapy drugs.[72] Especially, considering neutropenia as one main side effect of SN38, 4WJ-SN38 does not cause neutropenia since there is no reduction in the white blood cell count. These results demonstrate that SN38-conjugated RNA nanoparticles can mitigate abnormal conditions at the hematological level. These results further support that 4WJ-

https://doi.org/10.1021/acs.molpharmaceut.3c00845
Mol. Pharmaceutics XXXX, XXX, XXX−XXX

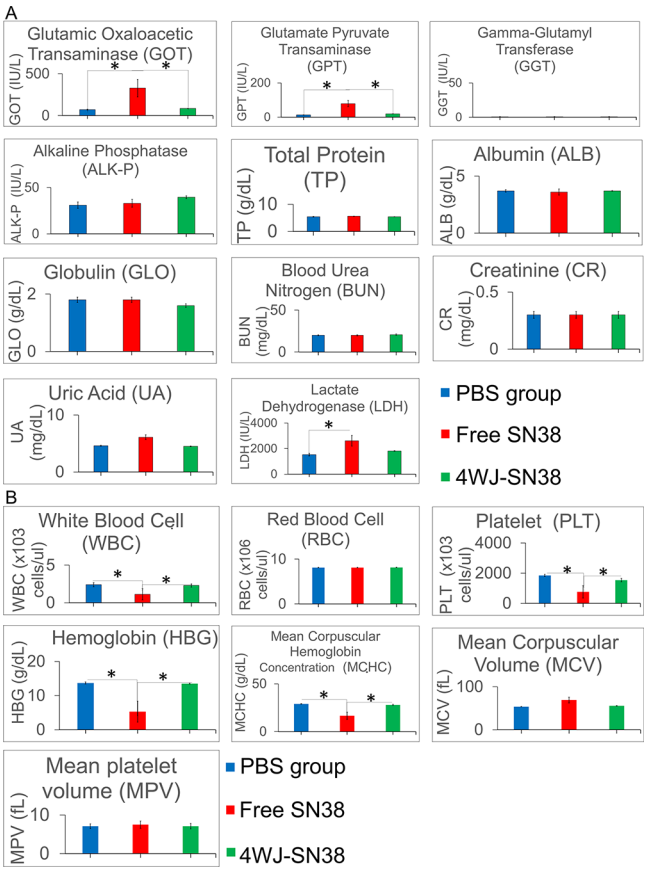

Figure 7. *In vivo* toxicity biomarkers study on 4WJ-SN38. (A) Serum biochemistry study, and (B) hematological study comparing PBS, SN38 free drug, and 4WJ-SN38 RNA nanoparticles. *$P < 0.05$.

SN38 RNA nanoparticles may improve the overall safety profile of SN38 for *in vivo* application, while further enhancing therapeutic delivery to tumors as we have previously demonstrated.

DISCUSSION

RNA nanotechnology is the bottom-up self-assembly of a nanometer-scale composed mainly of RNA.[15,31] However, such RNA nanoparticles can include, ligands, drugs, regulators, and image reporters.[13,73,74] RNA nanotechnology is analogous to "LEGO". The properties include (1) variety; (2) particles that can be constructed with controlled shape, size, and stoichiometry; (3) an assemble that can be achieved automatically; and (4) RNA that can be made thermodynamically, chemically, and enzymatically stable.[13,31] Recent worldwide use of mRNA vaccines for COVID-19[4−6] and the FDA approval of RNA drugs Onpattro, Oxlumo, and Givlaar[1−3] suggests that RNA therapeutics as the third milestone in pharmaceutical drug development is being realized.[12]

Clinical translation is an intermediate bridging between fundamental research and clinical practices. RNA nanoparticles remain stable *in vivo* while harboring therapeutic RNA or a high payload of chemical drugs such as SN38, accumulate at high levels in tumors, and provide active targeting by RNA aptamers or other ligands for delivery to tumors specifically. Herein, this report is a follow-up to long-lasting fundamental research in the field of RNA nanotechnology. The RNA complex with a defined structure, shape, size, stoichiometry, ligand, payload, and chemical composition for clinical application requires the consideration of (1) CMC production and shelf life; (2) IC50 and efficacy; and (3) LD50, side effects, and pathology. This study sheds light on further evaluation of the safety issue of RNA nanoparticles as therapeutic agents.

This report documents, in general, RNA nanoparticle safety, no damage to healthy organs, and no induction of cytokines or immune responses. The reasons for such high safety and low toxicity were also investigated.[13,14,45] The dynamic nature of RNA[75−77] leads to its motile and deformative behavior.[14] The near-neighbor principle in 2D and 3D structure folding,[78,79] the formation of pseudoknots of distal sequences,[80−82] the generation of thermodynamic motifs,[83] the breathing in base-pairing,[84,85] the induced-fit[86,87] and conformational capture property[88,89] all lead to a dynamic behavior with active motion of RNA. Actually, RNA has been recognized as a living organism and the origin of life.[90,91] Its deformable ability and penetrative capacity enable RNA to pass rapidly growing nascent blood capillary in tumor vasculature; thus, RNA can reach tumor vasculature spontaneously with high efficiency.[45] The elastic, rubbery, and amoeba properties are a factor in offering quick tumor-capillary penetration within 30 min of IV injection and fast renal excretion to urine after 30 min of IV injection.[45] RNA is an elastomer. Using optical tweezers, RNA was found to be an elastomer, as RNA nanoparticles could stretch under external force and can relax to their original size and shape repeatedly like rubber and amoeba.[45] The elastic[45,92] and motile properties make RNA nanoparticles change shapes to pass cancer blood capillary and enable the RNA/chemotherapeutics complex to enter tumor cells with increased tumor retention (5% of total dosage).[40] The 10 nm 4WJ can squeeze through and pass the 5.5 nm cutoff size of kidney globularia.[45,93] The rapid kidney clearance of the accessed RNA leads to fast body clearance and thus little toxicity. The biodistribution of RNA nanoparticles can be further improved by the incorporation of ligands for cancer targeting.[94] This special property resulted in highly efficient cancer targeting and rapid body clearance of RNA from the body without accumulation in organs or detectable toxicity.

Recently, protein corona formation at the surface of nanoparticles has been identified.[95] The protein corona formation can affect the biodistribution and safety of nanoparticles. Whether such a corona formation can occur with RNA nanoparticles is an intriguing question. The immediate effect of protein corona will be the change in morphology, size, and zeta potential of the RNA nanoparticles.[96,97] The shielding effect of protein corona could lead to a longer circulation time and a slow release of payload from the RNA nanoparticles as the corona may block the binding between RNA nanoparticles and RNase.[98] The attachment of the albumin onto the RNA nanoparticles may also increase the retention of RNA nanoparticles at the tumor sites;[99] however, it might also hinder the renal excretion and body clearance. The protein corona formation may further change the surface charge of the RNA nanoparticles,[96] and it might lead to an unfavorable healthy organ accumulation, which is negligible among negatively charged RNA nanoparticles.[37] To summarize, the protein corona formation may have both positive and negative effects on RNA nanoparticles. The application of artificial intelligence in understanding protein corona formation on RNA nanoparticles has also been reported,[95,100,101] and a more detailed investigation of the relationship between RNA nanoparticles and protein corona is important. Our

https://doi.org/10.1021/acs.molpharmaceut.3c00845
Mol. Pharmaceutics XXXX, XXX, XXX−XXX

preliminary studies indicated that serum albumin binding is RNA shape, size, and stoichiometry dependent, and the corona formation of 4WJ might not be a major concern (Archie Bhullar and Peixuan Guo, unpublished results).

CONCLUSIONS

The parameters of the pathology, safety, and side effects of RNA nanoparticles, including 3WJ and 4WJ bound to chemotherapeutic drugs, were investigated. Studies on *in vitro* and *in vivo* hemolysis, platelet aggregation, complement activation, plasma coagulation, interferon induction, cytokine induction, organ weight, H&E staining, serum biochemistry, and hematology revealed that no significant detected toxicity, side effects, or immune responses. To our best knowledge, this is the first comprehensive hemolysis level, platelet aggregation level, complement activation level, and plasma coagulation level study on RNA nanoparticles further advancing the field of RNA nanotechnology toward the clinic. immunogenicity level studies match our previous study. *In vivo* study further verifies the advantage of using RNA nanoparticles to deliver chemotherapeutics compared to free drug.

ASSOCIATED CONTENT

Supporting Information

The Supporting Information is available free of charge at https://pubs.acs.org/doi/10.1021/acs.molpharmaceut.3c00845.

Sterility and endotoxin check on 3WJ and 3WJ-FA-siRNA RNA nanoparticles and sequences of all RNA strands included in this study (PDF)

AUTHOR INFORMATION

Corresponding Authors

Peixuan Guo − *Division of Pharmaceutics and Pharmacology, College of Pharmacy, Center for RNA Nanotechnology and Nanomedicine, James Comprehensive Cancer Center, College of Medicine, and Dorothy M. Davis Heart and Lung Research Institute, College of Medicine, The Ohio State University, Columbus, Ohio 43210, United States*; orcid.org/0000-0001-5706-2833; Email: Guo.1091@OSU.edu

Yuan-Soon Ho − *Institute of Biochemistry and Molecular Biology, China Medical University, Taichung 406040, Taiwan*; Email: hoyuansn@cmu.edu.tw

Authors

Kai Jin − *Division of Pharmaceutics and Pharmacology, College of Pharmacy and Center for RNA Nanotechnology and Nanomedicine, The Ohio State University, Columbus, Ohio 43210, United States*

You-Cheng Liao − *Graduate Institute of Medical Sciences, College of Medicine, Taipei Medical University, Taipei 110031, Taiwan*

Tzu-Chun Cheng − *Institute of Biochemistry and Molecular Biology, China Medical University, Taichung 406040, Taiwan*

Xin Li − *Division of Pharmaceutics and Pharmacology, College of Pharmacy and Center for RNA Nanotechnology and Nanomedicine, The Ohio State University, Columbus, Ohio 43210, United States*

Wen-Jui Lee − *Division of Pharmaceutics and Pharmacology, College of Pharmacy and Center for RNA Nanotechnology and Nanomedicine, The Ohio State University, Columbus, Ohio 43210, United States*

Fengmei Pi − *Division of Pharmaceutics and Pharmacology, College of Pharmacy and Center for RNA Nanotechnology and Nanomedicine, The Ohio State University, Columbus, Ohio 43210, United States*

Daniel Jasinski − *Division of Pharmaceutics and Pharmacology, College of Pharmacy and Center for RNA Nanotechnology and Nanomedicine, The Ohio State University, Columbus, Ohio 43210, United States*

Li-Ching Chen − *Department of Biological Science and Technology, China Medical University, Taichung 406040, Taiwan*

Mitch A. Phelps − *Division of Pharmaceutics and Pharmacology, College of Pharmacy, The Ohio State University, Columbus, Ohio 43210, United States*

Complete contact information is available at: https://pubs.acs.org/10.1021/acs.molpharmaceut.3c00845

Author Contributions

Conceptualization, by P.G. and Y.S.H.; methodology, K.J., Y.C.L., T.C.C., X.L., W.J.L., F.P., D.J., and M.P.; investigation, Y.C.L., X.L., W.J.L., F.P., and D.J.; writing, K.J., and P.G.; figures by K.J., Y.C.L., P.G, L.C.C., and W.J.L.

Notes

The authors declare the following competing financial interest(s): P.G. is the consultant, licensor, and grantee of Oxford Nanopore Technologies as well as the cofounder and consultant of ExonanoRNA, LLC.

ACKNOWLEDGMENTS

The work was supported by the National Cancer Institute grant U01 CA207946 (P.G.) and NIH Eye Institute R01 EY031452 (P.G.). We thank the National Cancer Institute's Nanotechnology Characterization Laboratory (NCL) for characterizing the RNA nanoparticles. Some of the data, protocols, figures, and procedures described in this paper are provided by the NCL lab or derived from NCL protocols. The content is solely the authors' responsibility and does not necessarily represent the official views of NCL. Guo's Sylvan Frank Endowed Chair in Pharmaceutics and Drug Delivery position is supported by the Chen's Foundation. Part of the data was generated using the instruments and services at the Campus Microscopy and Imaging Facility, the Comprehensive Cancer Center of The Ohio State University. This facility is supported in part by grant P30 CA016058, National Cancer Institute, Bethesda, MD.

ABBREVIATIONS

3WJ, Three-way Junction; 4WJ, Four-way Junction; H&E, Hematoxylin and Eosin; 3WJ-FA-siRNA, three-way junction-Folic acid-Survivin siRNA RNA nanoparticles; 4WJ-SN38, four-way junction SN38-conjugated RNA nanoparticles; 2′F−C, 2′-Fluoro modified cytosine nucleotides; 2′F−U, 2′-Fluoro modified uracil nucleotides; CMH, cyanmethemoglobin; PRP, Platelet-rich plasma; PPP, plasma poor plasma; CVF, Cobra Venom Factor; APTT, activated partial thromboplastin time; PT, prothrombin time; LPS, lipopolysaccharides; IFN, Interferon; FFPE, formalin-fixed paraffin-embedded; FA, Folate Acid; EL, Endotoxin Limit; BLOD, below the limit of detection; GOT, Glutamic Oxaloacetic Transaminase; GPT,

Glutamate Pyruvate Transaminase; NCL, Nanotechnology Characterization Laboratory

REFERENCES

(1) Hoy, S. M. Patisiran: First Global Approval. *Drugs* **2018**, *78* (15), 1625−1631.

(2) Scott, L. J. Givosiran: First Approval. *Drugs* **2020**, *80* (3), 335−339.

(3) Scott, L. J.; Keam, S. J. Lumasiran: First Approval. *Drugs* **2021**, *81* (2), 277−282.

(4) Corbett, K. S.; Flynn, B.; Foulds, K. E.; Francica, J. R.; Boyoglu-Barnum, S.; Werner, A. P.; Flach, B.; O'Connell, S.; Bock, K. W.; Minai, M.; Nagata, B. M.; Andersen, H.; Martinez, D. R.; Noe, A. T.; Douek, N.; Donaldson, M. M.; Nji, N. N.; Alvarado, G. S.; Edwards, D. K.; Flebbe, D. R.; Lamb, E.; Doria-Rose, N. A.; Lin, B. C.; Louder, M. K.; O'Dell, S.; Schmidt, S. D.; Phung, E.; Chang, L. A.; Yap, C.; Todd, J. M.; Pessaint, L.; Van Ry, A.; Browne, S.; Greenhouse, J.; Putman-Taylor, T.; Strasbaugh, A.; Campbell, T. A.; Cook, A.; Dodson, A.; Steingrebe, K.; Shi, W.; Zhang, Y.; Abiona, O. M.; Wang, L.; Pegu, A.; Yang, E. S.; Leung, K.; Zhou, T.; Teng, I. T.; Widge, A.; Gordon, I.; Novik, L.; Gillespie, R. A.; Loomis, R. J.; Moliva, J. I.; Stewart-Jones, G.; Himansu, S.; Kong, W. P.; Nason, M. C.; Morabito, K. M.; Ruckwardt, T. J.; Ledgerwood, J. E.; Gaudinski, M. R.; Kwong, P. D.; Mascola, J. R.; Carfi, A.; Lewis, M. G.; Baric, R. S.; McDermott, A.; Moore, I. N.; Sullivan, N. J.; Roederer, M.; Seder, R. A.; Graham, B. S. Evaluation of the mRNA-1273 Vaccine against SARS-CoV-2 in Nonhuman Primates. *N. Engl. J. Med.* **2020**, *383*, 1544.

(5) Jackson, L. A.; Anderson, E. J.; Rouphael, N. G.; Roberts, P. C.; Makhene, M.; Coler, R. N.; McCullough, M. P.; Chappell, J. D.; Denison, M. R.; Stevens, L. J.; Pruijssers, A. J.; McDermott, A.; Flach, B.; Doria-Rose, N. A.; Corbett, K. S.; Morabito, K. M.; O'Dell, S.; Schmidt, S. D.; Swanson, P. A., 2nd; Padilla, M.; Mascola, J. R.; Neuzil, K. M.; Bennett, H.; Sun, W.; Peters, E.; Makowski, M.; Albert, J.; Cross, K.; Buchanan, W.; Pikaart-Tautges, R.; Ledgerwood, J. E.; Graham, B. S.; Beigel, J. H. An mRNA Vaccine against SARS-CoV-2 - Preliminary Report. *N. Engl. J. Med.* **2020**, *383* (20), 1920−1931.

(6) Pardi, N.; Hogan, M. J.; Porter, F. W.; Weissman, D. mRNA Vaccines - A New Era in Vaccinology. *Nat. Rev. Drug Discovery* **2018**, *17* (4), 261−279.

(7) Corbett, K. S.; Edwards, D. K.; Leist, S. R.; Abiona, O. M.; Boyoglu-Barnum, S.; Gillespie, R. A.; Himansu, S.; Schafer, A.; Ziwawo, C. T.; DiPiazza, A. T.; Dinnon, K. H.; Elbashir, S. M.; Shaw, C. A.; Woods, A.; Fritch, E. J.; Martinez, D. R.; Bock, K. W.; Minai, M.; Nagata, B. M.; Hutchinson, G. B.; Wu, K.; Henry, C.; Bahi, K.; Garcia-Dominguez, D.; Ma, L.; Renzi, I.; Kong, W. P.; Schmidt, S. D.; Wang, L.; Zhang, Y.; Phung, E.; Chang, L. A.; Loomis, R. J.; Altaras, N. E.; Narayanan, E.; Metkar, M.; Presnyak, V.; Liu, C.; Louder, M. K.; Shi, W.; Leung, K.; Yang, E. S.; West, A.; Gully, K. L.; Stevens, L. J.; Wang, N.; Wrapp, D.; Doria-Rose, N. A.; Stewart-Jones, G.; Bennett, H.; Alvarado, G. S.; Nason, M. C.; Ruckwardt, T. J.; McLellan, J. S.; Denison, M. R.; Chappell, J. D.; Moore, I. N.; Morabito, K. M.; Mascola, J. R.; Baric, R. S.; Carfi, A.; Graham, B. S. SARS-CoV-2 mRNA Vaccine Design Enabled by Prototype Pathogen Preparedness. *Nature* **2020**, 567−571.

(8) Guo, S.; Li, H.; Ma, M.; Fu, J.; Dong, Y.; Guo, P. Size, Shape, and Sequence-Dependent immunogenicity of RNA Nanoparticles. *Mol. Ther Nucleic Acids* **2017**, *9*, 399−408.

(9) Abdelmawla, S.; Guo, S.; Zhang, L.; Pulukuri, S. M.; Patankar, P.; Conley, P.; Trebley, J.; Guo, P.; Li, Q. X. Pharmacological characterization of chemically synthesized monomeric phi29 pRNA nanoparticles for systemic delivery. *Mol. Ther* **2011**, *19* (7), 1312−1322.

(10) Guo, S.; Vieweger, M.; Zhang, K.; Yin, H.; Wang, H.; Li, X.; Li, S.; Hu, S.; Sparreboom, A.; Evers, B. M.; Dong, Y.; Chiu, W.; Guo, P. Ultra-thermostable RNA nanoparticles for solubilizing and high-yield loading of paclitaxel for breast cancer therapy. *Nat. Commun.* **2020**, *11* (1), 972.

(11) LaFargue, C. J.; Amero, P.; Noh, K.; Mangala, L. S.; Wen, Y.; Bayraktar, E.; Umamaheswaran, S.; Stur, E.; Dasari, S. K.; Ivan, C.; Pradeep, S.; Yoo, W.; Lu, C.; Jennings, N. B.; Vathipadiekal, V.; Hu, W.; Chelariu-Raicu, A.; Ku, Z.; Deng, H.; Xiong, W.; Choi, H. J.; Hu, M.; Kiyama, T.; Mao, C. A.; Ali-Fehmi, R.; Birrer, M. J.; Liu, J.; Zhang, N.; Lopez-Berestein, G.; de Franciscis, V.; An, Z.; Sood, A. K. Overcoming adaptive resistance to anti-VEGF therapy by targeting CD5L. *Nat. Commun.* **2023**, *14* (1), 2407.

(12) Shu, Y.; Pi, F.; Sharma, A.; Rajabi, M.; Haque, F.; Shu, D.; Leggas, M.; Evers, B. M.; Guo, P. Stable RNA Nanoparticles as Potential New Generation Drugs for Cancer Therapy. *Adv. Drug Delivery Rev.* **2014**, *66*, 74−89.

(13) Binzel, D. W.; Li, X.; Burns, N.; Khan, E.; Lee, W. J.; Chen, L. C.; Ellipilli, S.; Miles, W.; Ho, Y. S.; Guo, P. Thermostability, Tunability, and Tenacity of RNA as Rubbery Anionic Polymeric Materials in Nanotechnology and Nanomedicine-Specific Cancer Targeting with Undetectable Toxicity. *Chem. Rev.* **2021**, *121* (13), 7398−7467.

(14) Li, X.; Bhullar, A. S.; Binzel, D. W.; Guo, P. The dynamic, motile and deformative properties of RNA nanoparticles facilitate the third milestone of drug development. *Adv. Drug Deliv Rev.* **2022**, *186*, No. 114316.

(15) Guo, P. The emerging field of RNA nanotechnology. *Nat. Nanotechnol* **2010**, *5* (12), 833−842.

(16) Rolband, L.; Beasock, D.; Wang, Y.; Shu, Y. G.; Dinman, J. D.; Schlick, T.; Zhou, Y.; Kieft, J. S.; Chen, S. J.; Bussi, G.; Oukhaled, A.; Gao, X.; Sulc, P.; Binzel, D.; Bhullar, A. S.; Liang, C.; Guo, P.; Afonin, K. A. Biomotors, viral assembly, and RNA nanobiotechnology: Current achievements and future directions. *Comput. Struct Biotechnol J.* **2022**, *20*, 6120−6137.

(17) Chandler, M.; Johnson, B.; Khisamutdinov, E.; Dobrovolskaia, M. A.; Sztuba-Solinska, J.; Salem, A. K.; Breyne, K.; Chammas, R.; Walter, N. G.; Contreras, L. M.; Guo, P.; Afonin, K. A. The International Society of RNA Nanotechnology and Nanomedicine (ISRNN): The Present and Future of the Burgeoning Field. *ACS Nano* **2021**, *15* (11), 16957−16973.

(18) Afonin, K. A.; Dobrovolskaia, M. A.; Ke, W.; Grodzinski, P.; Bathe, M. Critical review of nucleic acid nanotechnology to identify gaps and inform a strategy for accelerated clinical translation. *Adv. Drug Deliv Rev.* **2022**, *181*, No. 114081.

(19) Zhou, J.; Rossi, J. Aptamers as targeted therapeutics: current potential and challenges. *Nat. Rev. Drug Discovery* **2017**, *16* (3), 181−202.

(20) Afonin, K. A.; Cieply, D. J.; Leontis, N. B. Specific RNA self-assembly with minimal paranemic motifs. *J. Am. Chem. Soc.* **2008**, *130* (1), 93−102.

(21) Woodson, S. A. RNA folding and ribosome assembly. *Curr. Opin Chem. Biol.* **2008**, *12* (6), 667−673.

(22) Geary, C.; Chworos, A.; Verzemnieks, E.; Voss, N. R.; Jaeger, L. Composing RNA Nanostructures from a Syntax of RNA Structural Modules. *Nano Lett.* **2017**, *17* (11), 7095−7101.

(23) Grabow, W. W.; Zakrevsky, P.; Afonin, K. A.; Chworos, A.; Shapiro, B. A.; Jaeger, L. Self-assembling RNA Nanorings Based on RNAI/II Inverse Kissing Complexes. *Nano Lett.* **2011**, *11* (2), 878−887.

(24) Duckett, D. R.; Murchie, A. I.; Lilley, D. M. The Global Folding of Four-way Helical Junctions in RNA, Including that in U1 snRNA. *Cell* **1995**, *83* (6), 1027−1036.

(25) Afonin, K. A.; Viard, M.; Koyfman, A. Y.; Martins, A. N.; Kasprzak, W. K.; Panigaj, M.; Desai, R.; Santhanam, A.; Grabow, W. W.; Jaeger, L.; Heldman, E.; Reiser, J.; Chiu, W.; Freed, E. O.; Shapiro, B. A. Multifunctional RNA nanoparticles. *Nano Lett.* **2014**, *14* (10), 5662−5671.

(26) Li, J.; Wang, W.; He, Y.; Li, Y.; Yan, E. Z.; Zhang, K.; Irvine, D. J.; Hammond, P. T. Structurally Programmed Assembly of Translation Initiation Nanoplex for Superior mRNA Delivery. *ACS Nano* **2017**, *11* (3), 2531−2544.

(27) Boerneke, M. A.; Dibrov, S. M.; Hermann, T. Crystal-Structure-Guided Design of Self-Assembling RNA Nanotriangles. *Angew. Chem., Int. Ed. Engl.* **2016**, *55* (12), 4097−4100.

https://doi.org/10.1021/acs.molpharmaceut.3c00845
Mol. Pharmaceutics XXXX, XXX, XXX−XXX

(28) Malecka, E. M.; Woodson, S. A. Stepwise sRNA targeting of structured bacterial mRNAs leads to abortive annealing. *Mol. Cell* **2021**, *81* (9), 1988−1999.
(29) Lescoute, A.; Westhof, E. Topology of three-way junctions in folded RNAs. *RNA (New York, N.Y.)* **2006**, *12* (1), 83−93.
(30) Guo, P.; Zhang, C.; Chen, C.; Garver, K.; Trottier, M. Inter-RNA Interaction of Phage Phi29 pRNA to Form a Hexameric Complex for Viral DNA Transportation. *Mol. Cell* **1998**, *2* (1), 149−155.
(31) Shu, D.; Shu, Y.; Haque, F.; Abdelmawla, S.; Guo, P. Thermodynamically Stable RNA Three-way Junction for Constructing Multifunctional Nanoparticles for Delivery of Therapeutics. *Nat. Nanotechnol.* **2011**, *6* (10), 658−667.
(32) Xu, C.; Li, H.; Zhang, K.; Binzel, D. W.; Yin, H.; Chiu, W.; Guo, P. Photo-controlled Release of Paclitaxel and Model Drugs from RNA Pyramids. *Nano Res.* **2019**, *12*, 41−48.
(33) Shu, Y.; Haque, F.; Shu, D.; Li, W.; Zhu, Z.; Kotb, M.; Lyubchenko, Y.; Guo, P. Fabrication of 14 different RNA nanoparticles for specific tumor targeting without accumulation in normal organs. *RNA (New York, N.Y.)* **2013**, *19* (6), 767−777.
(34) Yin, H.; Wang, H.; Li, Z.; Shu, D.; Guo, P. RNA Micelles for the Systemic Delivery of Anti-miRNA for Cancer Targeting and Inhibition without Ligand. *ACS Nano* **2019**, *13* (1), 706−717.
(35) Li, H.; Zhang, K.; Pi, F.; Guo, S.; Shlyakhtenko, L.; Chiu, W.; Shu, D.; Guo, P. Controllable Self-Assembly of RNA Tetrahedrons with Precise Shape and Size for Cancer Targeting. *Adv. Mater.* **2016**, *28* (34), 7501−7507.
(36) Guo, P.; Coban, O.; Snead, N. M.; Trebley, J.; Hoeprich, S.; Guo, S.; Shu, Y. Engineering RNA for targeted siRNA delivery and medical application. *Adv. Drug Deliv Rev.* **2010**, *62* (6), 650−666.
(37) Shu, Y.; Yin, H.; Rajabi, M.; Li, H.; Vieweger, M.; Guo, S.; Shu, D.; Guo, P. RNA-based micelles: A novel platform for paclitaxel loading and delivery. *J. Controlled Release* **2018**, *276*, 17−29.
(38) Zhang, Y.; Leonard, M.; Shu, Y.; Yang, Y.; Shu, D.; Guo, P.; Zhang, X. Overcoming Tamoxifen Resistance of Human Breast Cancer by Targeted Gene Silencing Using Multifunctional pRNA Nanoparticles. *ACS Nano* **2017**, *11* (1), 335−346.
(39) Rychahou, P.; Haque, F.; Shu, Y.; Zaytseva, Y.; Weiss, H. L.; Lee, E. Y.; Mustain, W.; Valentino, J.; Guo, P.; Evers, B. M. Delivery of RNA nanoparticles into colorectal cancer metastases following systemic administration. *ACS Nano* **2015**, *9* (2), 1108−1116.
(40) Wang, H.; Guo, P. Radiolabeled RNA Nanoparticles for Highly Specific Targeting and Efficient Tumor Accumulation with Favorable *In vivo* Biodistribution. *Mol. Pharmaceutics* **2021**, *18* (8), 2924−2934.
(41) Binzel, D. W.; Shu, Y.; Li, H.; Sun, M.; Zhang, Q.; Shu, D.; Guo, B.; Guo, P. Specific Delivery of MiRNA for High Efficient Inhibition of Prostate Cancer by RNA Nanotechnology. *Molecular therapy: the journal of the American Society of Gene Therapy* **2016**, *24* (7), 1267−1277.
(42) Cui, D.; Zhang, C.; Liu, B.; Shu, Y.; Du, T.; Shu, D.; Wang, K.; Dai, F.; Liu, Y.; Li, C.; Pan, F.; Yang, Y.; Ni, J.; Li, H.; Brand-Saberi, B.; Guo, P. Regression of Gastric Cancer by Systemic Injection of RNA Nanoparticles Carrying both Ligand and siRNA. *Sci. Rep.* **2015**, *5*, 10726.
(43) Shu, D.; Li, H.; Shu, Y.; Xiong, G.; Carson, W. E., 3rd; Haque, F.; Xu, R.; Guo, P. Systemic Delivery of Anti-miRNA for Suppression of Triple Negative Breast Cancer Utilizing RNA Nanotechnology. *ACS Nano* **2015**, *9* (10), 9731−9740.
(44) Matsuda, A.; Patel, T. Milk-derived Extracellular Vesicles for Therapeutic Delivery of Small Interfering RNAs. *Methods Mol. Biol.* **2018**, *1740*, 187−197.
(45) Ghimire, C.; Wang, H.; Li, H.; Vieweger, M.; Xu, C.; Guo, P. RNA Nanoparticles as Rubber for Compelling Vessel Extravasation to Enhance Tumor Targeting and for Fast Renal Excretion to Reduce Toxicity. *ACS Nano* **2020**, *14* (10), 13180−13191.
(46) Wang, H.; Ellipilli, S.; Lee, W. J.; Li, X.; Vieweger, M.; Ho, Y. S.; Guo, P. Multivalent rubber-like RNA nanoparticles for targeted co-delivery of paclitaxel and MiRNA to silence the drug efflux transporter and liver cancer drug resistance. *J. Controlled Release* **2021**, *330*, 173−184.
(47) Chiran, G.; Peixuan, G. Optical tweezer and TIRF microscopy for single molecule manipulation of RNA/DNA Nanostructures including their rubbery property and single molecule counting. *Biophysics Reports* **2021**, *7* (6), 449−474.
(48) Liu, J.; Guo, S.; Cinier, M.; Shlyakhtenko, L. S.; Shu, Y.; Chen, C.; Shen, G.; Guo, P. Fabrication of Stable and RNase-Resistant RNA Nanoparticles Active in Gearing the Nanomotors for Viral DNA Packaging. *ACS Nano* **2011**, *5* (1), 237−246.
(49) Neun, B. W.; Ilinskaya, A. N.; Dobrovolskaia, M. A. Updated Method for *In vitro* Analysis of Nanoparticle Hemolytic Properties. *Methods Mol. Biol.* **2018**, *1682*, 91−102.
(50) Malinauskas, R. A. *Plasma hemoglobin measurement techniques for the in vitro evaluation of blood damage caused by medical devices*. (0160−564X (Print)).
(51) Rodriguez, J.; Cedrone, E.; Neun, B.; Dobrovolskaia, M. *NCL Method ITA-2.2*. 2020.
(52) Neun, B. W.; Ilinskaya, A. N.; Dobrovolskaia, M. A. Analysis of Complement Activation by Nanoparticles. *Methods Mol. Biol.* **2018**, *1682*, 149−160.
(53) Cedrone, E.; Potter, T.; Neun, B.; Dobrovolskaia, M. *NCL Method ITA-12*. 2020.
(54) Potter, T. M.; Neun, B. W.; Rodriguez, J. C.; Ilinskaya, A. N.; Dobrovolskaia, M. A. Analysis of Pro-inflammatory Cytokine and Type II Interferon Induction by Nanoparticles. *Methods Mol. Biol.* **2018**, *1682*, 173−187.
(55) Neun, B.; Rodriguez, J.; Potter, T.; Ilinskaya, A.; Dobrovolskaia, M. *NCL Method ITA-25*. 2020.
(56) Cedrone, E.; Potter, T.; Neun, B.; Tyler, A.; Dobrovolskaia, M. *NCL Method ITA-27*. 2021.
(57) Xu, Y.; Pang, L.; Wang, H.; Xu, C.; Shah, H.; Guo, P.; Shu, D.; Qian, S. Y. Specific delivery of delta-5-desaturase siRNA via RNA nanoparticles supplemented with dihomo-γ-linolenic acid for colon cancer suppression. *Redox Biology* **2019**, *21*, No. 101085.
(58) Lin, Y. S.; Haynes, C. L. Impacts of mesoporous silica nanoparticle size, pore ordering, and pore integrity on hemolytic activity. *J. Am. Chem. Soc.* **2010**, *132* (13), 4834−4842.
(59) Fornaguera, C.; Caldero, G.; Mitjans, M.; Vinardell, M. P.; Solans, C.; Vauthier, C. Interactions of PLGA nanoparticles with blood components: protein adsorption, coagulation, activation of the complement system and hemolysis studies. *Nanoscale* **2015**, *7* (14), 6045−6058.
(60) Radomski, A.; Jurasz, P.; Alonso-Escolano, D.; Drews, M.; Morandi, M.; Malinski, T.; Radomski, M. W. Nanoparticle-induced platelet aggregation and vascular thrombosis. *Br. J. Pharmacol.* **2005**, *146* (6), 882−893.
(61) Guidetti, G. F.; Consonni, A.; Cipolla, L.; Mustarelli, P.; Balduini, C.; Torti, M. Nanoparticles induce platelet activation *in vitro* through stimulation of canonical signalling pathways. *Nanomed-Nanotechnol* **2012**, *8* (8), 1329−1336.
(62) Aggarwal, P.; Hall, J. B.; McLeland, C. B.; Dobrovolskaia, M. A.; McNeil, S. E. Nanoparticle interaction with plasma proteins as it relates to particle biodistribution, biocompatibility and therapeutic efficacy. *Adv. Drug Delivery Rev.* **2009**, *61* (6), 428−437.
(63) La-Beck, N. M.; Islam, M. R.; Markiewski, M. M. Nanoparticle-Induced Complement Activation: Implications for Cancer Nanomedicine. *Front. Immunol.* **2021**, *11*, No. 603039.
(64) Pannuzzo, M.; Esposito, S.; Wu, L. P.; Key, J.; Aryal, S.; Celia, C.; di Marzio, L.; Moghimi, S. M.; Decuzzi, P. Overcoming Nanoparticle-Mediated Complement Activation by Surface PEG Pairing. *Nano Lett.* **2020**, *20* (6), 4312−4321.
(65) Rehwinkel, J.; Gack, M. U. RIG-I-like receptors: their regulation and roles in RNA sensing. *Nat. Rev. Immunol* **2020**, *20* (9), 537−551.
(66) Khisamutdinov, E. F.; Li, H.; Jasinski, D. L.; Chen, J.; Fu, J.; Guo, P. X. Enhancing immunomodulation on innate immunity by shape transition among RNA triangle, square and pentagon nanovehicles. *Nucleic Acids Res.* **2014**, *42* (15), 9996−10004.

https://doi.org/10.1021/acs.molpharmaceut.3c00845
Mol. Pharmaceutics XXXX, XXX, XXX−XXX

(67) de Man, F. M.; Goey, A. K. L.; van Schaik, R. H. N.; Mathijssen, R. H. J.; Bins, S. Individualization of Irinotecan Treatment: A Review of Pharmacokinetics, Pharmacodynamics, and Pharmacogenetics. *Clinical Pharmacokinetics* **2018**, *57* (10), 1229−1254.
(68) Vejjasilpa, K.; Nasongkla, N.; Manaspon, C.; Larbcharoensub, N.; Boongird, A.; Hongeng, S.; Israsena, N. Antitumor efficacy and intratumoral distribution of SN-38 from polymeric depots in brain tumor model. *Exp Biol. Med. (Maywood)* **2015**, *240* (12), 1640−1647.
(69) Han, J.; Zhang, J.; Zhang, C. Irinotecan-Induced Steatohepatitis: Current Insights. *Front. Oncol* **2021**, *11*, No. 754891.
(70) Danpure, C. J. Lactate dehydrogenase and cell injury. *Cell Biochem Funct* **1984**, *2* (3), 144−148.
(71) Pal, A.; Khan, S.; Wang, Y. F.; Kamath, N.; Sarkar, A. K.; Ahmad, A.; Sheikh, S.; Ali, S.; Carbonaro, D.; Zhang, A.; Ahmad, I. Preclinical safety, pharmacokinetics and antitumor efficacy profile of liposome-entrapped SN-38 formulation. *Anticancer Res.* **2005**, *25* (1A), 331−341.
(72) Groopman, J. E.; Itri, L. M. Chemotherapy-induced anemia in adults: incidence and treatment. *J. Natl. Cancer Inst* **1999**, *91* (19), 1616−1634.
(73) Jasinski, D.; Haque, F.; Binzel, D. W.; Guo, P. Advancement of the Emerging Field of RNA Nanotechnology. *ACS Nano* **2017**, *11* (2), 1142−1164.
(74) Li, H.; Lee, T.; Dziubla, T.; Pi, F.; Guo, S.; Xu, J.; Li, C.; Haque, F.; Liang, X. J.; Guo, P. RNA as a Stable Polymer to Build Controllable and Defined Nanostructures for Material and Biomedical Applications. *Nano Today* **2015**, *10* (5), 631−655.
(75) Al-Hashimi, H. M.; Walter, N. G. RNA dynamics: it is about time. *Curr. Opin Struct Biol.* **2008**, *18* (3), 321−329.
(76) Hall, K. B. RNA in motion. *Curr. Opin Chem. Biol.* **2008**, *12* (6), 612−618.
(77) Hansen, A. L.; Al-Hashimi, H. M. Dynamics of large elongated RNA by NMR carbon relaxation. *J. Am. Chem. Soc.* **2007**, *129* (51), 16072−16082.
(78) Wang, Y.; Wang, Z.; Wang, Y.; Liu, T.; Zhang, W. The nearest neighbor and next nearest neighbor effects on the thermodynamic and kinetic properties of RNA base pair. *J. Chem. Phys.* **2018**, *148* (4), No. 045101.
(79) Zuber, J.; Cabral, B. J.; McFadyen, I.; Mauger, D. M.; Mathews, D. H. Analysis of RNA nearest neighbor parameters reveals interdependencies and quantifies the uncertainty in RNA secondary structure prediction. *RNA* **2018**, *24* (11), 1568−1582.
(80) Cao, S.; Chen, S. J. Predicting RNA Pseudoknot Folding Thermodynamics. *Nucleic Acids Res.* **2006**, *34* (9), 2634−2652.
(81) Felden, B.; Florentz, C.; Giege, R.; Westhof, E. A Central Pseudoknotted Three-way Junction Imposes tRNA-like Mimicry and the Orientation of Three 5′ Upstream pseudoknots in the 3′ Terminus of Tobacco Mosaic Virus RNA. *RNA* **1996**, *2* (3), 201−212.
(82) Giedroc, D. P.; Cornish, P. V. Frameshifting RNA pseudoknots: structure and mechanism. *Virus Res.* **2009**, *139* (2), 193−208.
(83) Ferner, J.; Villa, A.; Duchardt, E.; Widjajakusuma, E.; Wohnert, J.; Stock, G.; Schwalbe, H. NMR and MD studies of the temperature-dependent dynamics of RNA YNMG-tetraloops. *Nucleic Acids Res.* **2008**, *36* (6), 1928−1940.
(84) Williams, A. A.; Darwanto, A.; Theruvathu, J. A.; Burdzy, A.; Neidigh, J. W.; Sowers, L. C. Impact of Sugar Pucker on Base Pair and Mispair Stability. *Biochemistry* **2009**, *48* (50), 11994−12004.
(85) Dubey, A.; Bandyopadhyay, M. DNA breathing dynamics under periodic forcing: Study of several distribution functions of relevant Brownian functionals. *Phys. Rev. E* **2019**, *100* (5−1), No. 052107.
(86) Ilin, S.; Hoskins, A.; Ohlenschlager, O.; Jonker, H. R.; Schwalbe, H.; Wohnert, J. Domain reorientation and induced fit upon RNA binding: solution structure and dynamics of ribosomal protein L11 from Thermotoga maritima. *Chembiochem* **2005**, *6* (9), 1611−1618.
(87) Noeske, J.; Buck, J.; Furtig, B.; Nasiri, H. R.; Schwalbe, H.; Wohnert, J. Interplay of 'induced fit' and preorganization in the ligand induced folding of the aptamer domain of the guanine binding riboswitch. *Nucleic Acids Res.* **2006**, *35* (2), 572−583.
(88) Haller, A.; Rieder, U.; Aigner, M.; Blanchard, S. C.; Micura, R. Conformational capture of the SAM-II riboswitch. *Nat. Chem. Biol.* **2011**, *7* (6), 393−400.
(89) Lee, S. W.; Zhao, L.; Pardi, A.; Xia, T. Ultrafast dynamics show that the theophylline and 3-methylxanthine aptamers employ a conformational capture mechanism for binding their ligands. *Biochemistry* **2010**, *49* (13), 2943−2951.
(90) Fine, J. L.; Pearlman, R. E. On the origin of life: an RNA-focused synthesis and narrative. *RNA* **2023**, *29* (8), 1085−1098.
(91) Higgs, P. G.; Lehman, N. The RNA World: molecular cooperation at the origins of life. *Nat. Rev. Genet* **2015**, *16* (1), 7−17.
(92) Chiu, H. C.; Koh, K. D.; Evich, M.; Lesiak, A. L.; Germann, M. W.; Bongiorno, A.; Riedo, E.; Storici, F. RNA Intrusions Change DNA Elastic Properties and Structure. *Nanoscale* **2014**, *6* (17), 10009−10017.
(93) Piao, X.; Wang, H.; Binzel, D. W.; Guo, P. Assessment and Comparison of Thermal Stability of Phosphorothioate-DNA, DNA, RNA, 2'-F RNA, and LNA in the Context of Phi29 pRNA 3WJ. *RNA* **2018**, *24* (1), 67−76.
(94) Li, X.; Jin, K.; Cheng, T. C.; Liao, Y. C.; Lee, W. J.; Bhullar, A. S.; Chen, L. C.; Rychahou, P.; Phelps, M. A.; Ho, Y. S.; Guo, P. RNA 4WJ for Spontaneous Cancer-Targeting, Effective Tumor-Regression, Metastasis Suppression, Fast Renal Excretion and Undetectable Toxicity. *Biomaterials* **2023**, 122432.
(95) Mahmoudi, M.; Landry, M. P.; Moore, A.; Coreas, R. The protein corona from nanomedicine to environmental science. *Nat. Rev. Mater.* **2023**, *8*, 422−438.
(96) Pinals, R. L.; Chio, L.; Ledesma, F.; Landry, M. P. Engineering at the nano-bio interface: harnessing the protein corona towards nanoparticle design and function. *Analyst* **2020**, *145* (15), 5090−5112.
(97) Li, Y.; Lee, J.-S. Insights into Characterization Methods and Biomedical Applications of Nanoparticle−Protein Corona. *Materials* **2020**, *13*, 3093.
(98) Wu, J.; Peng, H.; Lu, X.; Lai, M.; Zhang, H.; Le, X. C. Binding-Mediated Formation of Ribonucleoprotein Corona for Efficient Delivery and Control of CRISPR/Cas9. *Angew. Chem., Int. Ed. Engl.* **2021**, *60* (20), 11104−11109.
(99) Lorents, A.; Maloverjan, M.; Padari, K.; Pooga, M. Internalisation and Biological Activity of Nucleic Acids Delivering Cell-Penetrating Peptide Nanoparticles Is Controlled by the Biomolecular Corona. *Pharmaceuticals* **2021**, *14*, 667.
(100) Duan, Y.; Coreas, R.; Liu, Y.; Bitounis, D.; Zhang, Z.; Parviz, D.; Strano, M.; Demokritou, P.; Zhong, W. Prediction of protein corona on nanomaterials by machine learning using novel descriptors. *NanoImpact* **2020**, *17*, No. 100207.
(101) Hajipour, M. J.; Safavi-Sohi, R.; Sharifi, S.; Mahmoud, N.; Ashkarran, A. A.; Voke, E.; Serpooshan, V.; Ramezankhani, M.; Milani, A. S.; Landry, M. P.; Mahmoudi, M. An Overview of Nanoparticle Protein Corona Literature. *Small* **2023**, *19* (36), No. e2301838.

https://doi.org/10.1021/acs.molpharmaceut.3c00845
Mol. Pharmaceutics XXXX, XXX, XXX−XXX